

Brushite foams—the effect of Tween® 80 and Pluronic® F-127 on foam porosity and mechanical properties

Johanna Unosson,^{1,2} Edgar B. Montufar,^{3,4} Håkan Engqvist,^{1,2} Maria-Pau Ginebra,^{3,4} Cecilia Persson^{1,2}

¹Department of Engineering Sciences, Division of Applied Materials Science, Uppsala University, Sweden

²Department of Engineering Sciences, Uppsala University, Sweden

³Biomaterials, Biomechanics and Tissue Engineering Group, Department of Materials Science and Metallurgy, Technical University of Catalonia (UPC), ETSEIB, Spain

⁴Biomedical Research Networking Center in Bioengineering, Biomaterials and Nanomedicine (CIBER-BBN), Spain

Received 22 May 2014; revised 19 November 2014; accepted 2 December 2014

Published online 23 January 2015 in Wiley Online Library (wileyonlinelibrary.com). DOI: 10.1002/jbm.b.33355

Abstract: Resorbable calcium phosphate based bone void fillers should work as temporary templates for new bone formation. The incorporation of macropores with sizes of 100–300 μm has been shown to increase the resorption rate of the implant and speed up bone ingrowth. In this work, macroporous brushite cements were fabricated through foaming of the cement paste, using two different synthetic surfactants, Tween® 80 and Pluronic® F-127. The macropores formed in the Pluronic samples were both smaller and less homogeneously distributed compared with the pores formed in the Tween samples. The porosity and compressive strength (CS) were comparable to previously developed hydroxyapatite foams. The cement foam containing Tween, 0.5M citric acid in the liquid, 1 mass% of diso-

dium dihydrogen pyrophosphate mixed in the powder and a liquid to powder ratio of 0.43 mL/g, showed the highest porosity values (76% total and 56% macroporosity), while the CS was >1 MPa, that is, the hardened cement could be handled without rupture of the foamed structure. The investigated brushite foams show potential for future clinical use, both as bone void fillers and as scaffolds for *in vitro* bone regeneration. © 2015 The Authors. Journal of Biomedical Materials Research Part B: Applied Biomaterials Published by Wiley Periodicals, Inc. J Biomed Mater Res Part B: Appl Biomater, 104B: 67–77, 2016.

Key Words: Brushite, foam, Tween®, 80, Pluronic®, F-127, porosity, strength, setting time

How to cite this article: Unosson J, Montufar EB, Engqvist H, Ginebra M-P, Persson C. 2016. Brushite foams—the effect of Tween® 80 and Pluronic® F-127 on foam porosity and mechanical properties. J Biomed Mater Res Part B 2016;104B:67–77.

INTRODUCTION

The development of degradable synthetic materials intended for bone void filling has been a focus of materials research for several years, mainly due to the numerous potential clinical applications; for example, bone voids due to osteosarcoma, non-union of fractures, implant fixation, bone loss due to infection, etc. Calcium phosphates^{1,2} are one group of synthetic materials used in these applications that are both degradable and biocompatible. Furthermore, they have the advantage of having a chemical composition similar to the mineral phase of bone. To reduce the risk of implant failure, an implanted material must have a rapid resorption rate that matches the rapid formation of new bone. Several studies have shown that the introduction of macropores in the material can increase the resorption rate.³ Moreover, it is

known that pore sizes >100 μm are required for a good bone ingrowth, while sizes above 300 μm can enhance capillary and bone formation.⁴

Self-setting macroporous calcium phosphates can be obtained either through foaming of a calcium phosphate cement (CPC), a method which has been extensively studied for hydroxyapatite (HA) cements by Ginebra et al.,⁵ or through the use of a sacrificial phase.^{6–10} Cement foams have mainly been produced through foaming of a liquid that contains a foaming agent (surfactant), either through the introduction of pressurized air¹¹ or through mechanical foaming, for example, stirring.^{5,12,13} The advantage of mechanical foaming over the other alternatives is the generally better distribution of the pores and the higher degree of pore interconnectivity.^{3,7,8,12} However, most hitherto

Correspondence to: J. Unosson; e-mail: johanna.unosson@angstrom.uu.se

Contract grant sponsor: FP7 NMP project Biodesign

Contract grant sponsor: The Swedish Foundation for International Cooperation in Research and Higher Education (STINT); contract grant number: GA IG2011-2047

Contract grant sponsor: Swedish Research Council; contract grant numbers: GA 621–2011–6258 and GA 621–2011–3399

Contract grant sponsor: Spanish Government; contract grant number: MAT 2012–38438-C03-01

Contract grant sponsor: Generalitat de Catalunya

investigated macroporous CPCs have been derived from cements with HA as the set phase, with only two exceptions for brushite cements.^{14,15} The acidic CPCs, with brushite (and in a few cases monetite^{14,16}) as the set phase have the advantage of a greater resorption rate than HA cements, due both to a higher dissolution rate at physiological pH and to a faster active degradation by cells.¹⁷⁻¹⁹ The faster rate of degradation makes them particularly appropriate for bone void filling. The incorporation of macropores is expected to further increase the rate of resorption and replacement of bone, especially if the pores are larger than 100 μm .⁴ The rapidly degrading macroporous CPCs could furthermore be of preference in other applications, such as structural templates for *in vitro* bone formation.²⁰ However, highly porous HA cements are often fragile, thus the bulk material must have a high compressive strength (CS), or the fabricated scaffold will be extremely fragile.^{3,5,6,21} This is a challenge with brushite cements because, generally, they are not as strong as HA cements. We have recently reported a strategy to improve the mechanical properties of brushite cements,²² and strengths comparable to HA cements have been achieved. It is thus of high interest to investigate whether it is possible to obtain brushite foams starting from the brushite cement formulation previously studied.^{22,23}

A range of surfactants have been used as foaming agents for HA cements, both natural (e.g., albumen^{3,5} and gelatine^{12,13}) and synthetic [e.g., Polysorbate 80 (commercially known as Tween® 80)^{24,25}]. Montufar et al.²⁴ showed that Tween gave larger and more interconnected pores than gelatine. Gelatine, on the other hand, increased the injectability and cohesion of the foams. However, the mixing and foaming needed to be performed at 50 °C, due to the gelling properties of gelatine below 37 °C. Montufar et al.^{24,25} have furthermore shown that low concentrations of Tween (0.5–1 mass% in the liquid) are sufficient to obtain stable HA foams. Tween is a nonionic surfactant derived from polyethoxylated sorbitan (hydrophilic block) and oleic acid (hydrophobic tail)^{26,27}. In addition to its efficiency as foaming agent, Tween has the added advantage of stable foaming properties with regard to pH changes, longer shelf life compared with natural foaming agents, and a lack of immunogenicity. Another possible synthetic non-ionic surfactant that is approved by the FDA, and has been used in several biological applications such as drug delivery systems, is Pluronic® F-127.²⁸ Pluronic is a triblock copolymer consisting of a central hydrophobic block of polypropylene glycol flanked by two hydrophilic blocks of polyethylene glycol.²⁹ An important property of Pluronic is its inverse thermoreversible gelling ability. In other words, when temperature increases to body temperature Pluronic (>20 mass%) forms a gel due to the lower solubility of polypropylene glycol at high temperatures.²⁸ Although this characteristic can improve the cohesion of injectable foams, Pluronic has not previously been tested for use as a foaming agent in cement formulations.

In this study, brushite foams were evaluated using two synthetic surfactants, Tween and Pluronic. The effect of fabrication conditions, such as the liquid to powder ratio and the addition of various setting retardants, on the porosity,

microstructure, setting times, and mechanical properties of the foams was also analyzed, to assess the potential clinical applications of brushite foams.

MATERIALS AND METHODS

Foam preparation

The powder used to prepare the cements contained β -tricalcium phosphate (β -TCP, >96%, 21218, Sigma Aldrich, St. Louis, MO) and monocalcium phosphate monohydrate (>98%, sieved to <75 μm , CA0211005P, Scharlau, Barcelona, Spain) in a 55:45% molar ratio.²² The average particle size of the β -TCP was 13.6 (\pm 0.1) μm , as measured by laser diffraction (Mastersizer X, Malvern Instruments, Malvern, UK). Disodium dihydrogen pyrophosphate (SPP, >99%, 71501, Sigma Aldrich) was used as a setting retardant in three concentrations; 1, 2, and 3 mass% of the powder.

The liquid consisted of either distilled water (Milli-Q, Merck Millipore, Billerica, MA) or citric acid (0.5 M, aq), mixed with 1 mass% of either Tween® 80 (Tween, P4780, Sigma Aldrich) or Pluronic® F-127 (Pluronic, P2443, Sigma Aldrich). When a low content of SPP was used (1 mass%) the foams set in a few minutes, and an additional setting retardant (citric acid, CA, 0.5M, aq, pH = 1.55 \pm 0.01, C0759, Sigma Aldrich), was therefore used as the mixing liquid to prolong the setting time of these compositions. The three retardant combinations (1 mass% SPP + citric acid, 2 mass% SPP + water, 3 mass% SPP + water) gave brushite foams with different setting times. Since cements with a longer setting time require less liquid to achieve workable foams, the liquid to powder ratio (*L/P*) was varied between the compositions. The samples are here after named X-0.YY-Z-L, where X indicates if Tween (T) or Pluronic (P) is used, 0.YY is the *L/P* ratio, Z is the mass% of SPP in the powder and L is the liquid used with C indicating 0.5M citric acid, and W indicating distilled water.

The liquid (3 mL) was mechanically foamed using a custom-made mixer (stainless steel blade adapted to a Dremel 4000, Robert Bosch Tool Corporation, Mount Prospect, IL) for 30 s in a clean container, after which 2 g of the foam was added to the correct amount of preblended powder. The powder was carefully incorporated into the liquid foam for 40 s using a spatula, after which the cement foam was molded in either polytetrafluoreten (PTFE) or rubber molds (Microset 101XF, Microset Products, Nuneaton, UK). The foams were stored at 37 °C and 100% humidity until approximately half of the initial setting time (IST) had passed, after which they were placed in phosphate buffered saline (PBS, 00-3002, GIBCO, 0.01M phosphate buffer, 0.0027M potassium chloride, and 0.140M sodium chloride, pH = 7.4, Thermo Fisher Scientific, Waltham, MA) at 37 °C for 24 h. Nonfoamed samples for intrinsic porosity evaluation were prepared and treated in the same manner as the foams, but without the foaming step.

Liquid foam characterization

The foamability of the liquid foams was characterized by measuring the increase in volume of the surfactant solution during the foaming process³⁰ and was calculated according

to Eq. (1), where F is the foamability, V_f is the volume after foaming and V_i is the initial volume of the surfactant solution. The results are expressed as average and standard deviation of three samples.

$$F = \frac{(V_f - V_i)}{V_i} \quad (1)$$

The microstructures of the liquid foams were furthermore studied 1, 3, and 6 min after foaming using an optical microscope (SZX16, Olympus, Tokyo, Japan).

Setting time

The setting time of the brushite foams was measured using the Gilmore needle testing method according to ASTM C266-99.³¹ The foamed cements were stored at 37 °C and 100% humidity until a visible mark could no longer be seen on the sample when a weight of 113.4 (± 0.5) g with a tip diameter of 2.12 (± 0.05) mm (equivalent of a load of ~ 0.3 MPa) was carefully placed on the surface. This is defined as the IST in the standard and was measured for 15 samples per group. Final setting time is defined by the standard as the time it takes for the cement to withstand a load equivalent to ~ 5 MPa,³¹ which most of the compositions within this study never reached. This value was, hence, not measured.

Porosity and microstructure

PTFE molds measuring 6 mm diameter and 6 mm height were used to produce samples for porosity measurements. Six samples were cured together in 30 mL of PBS. The samples were demolded and dried in vacuum over silica gel beads at room temperature for three days before the porosity was measured. The average skeletal density was determined with helium pycnometry (AccuPyc 1340, Micromeritics, Norcross, GA) using 20 purges and 10 runs. The mass and outer dimensions of each sample were measured to achieve the apparent density, after which the total porosity was calculated using Eq. (2). To calculate the macroporosity, the apparent density of the nonfoamed samples was measured and the macroporosity was calculated according to Eq. (3), previously described thoroughly by Takagi and Chow,⁸ where Φ_{tot} is the total porosity, Φ_{macro} is the macroporosity, ρ_{af} is the apparent density of the foamed cement, ρ_{anf} is the apparent density of the nonfoamed cement, and ρ_s is the skeletal density.

$$\Phi_{\text{tot}} = \left(1 - \frac{\rho_{\text{af}}}{\rho_s} \right) \quad (2)$$

$$\Phi_{\text{macro}} = \left(1 - \frac{\rho_{\text{af}}}{\rho_{\text{anf}}} \right) \quad (3)$$

The open porosity and the entrance pore size distribution between 0.006 and 360 μm were measured by MIP (AutoPore IV 9500, Micromeritics), in cylindrical specimens (6 mm diameter and 6 mm height). Samples ($n = 3$) with the highest and the lowest L/P ratio with 1 mass% SPP foamed with Tween were analyzed. Pores with an entrance

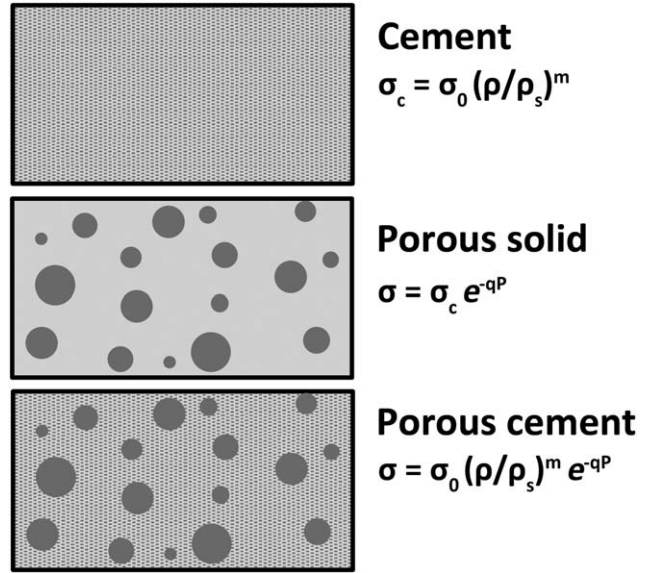


FIGURE 1. Illustration of the model used for the relationship between CS and porosity.

pore diameter $> 5 \mu\text{m}$ were defined as macropores. The microstructure of the samples was studied on cross sections with scanning electron microscopy (SEM, Neon40, Zeiss, Oberkochen, Germany). To decrease sample charging during analysis, a thin gold/palladium layer was deposited on the sample surface through physical vapor deposition (K950X Turbo Evaporator, Quorum Technologies, Laughton, UK) before analysis. The interconnectivity of 11 samples per group was furthermore analyzed with image analysis using ImageJ (National Institutes of Health, Bethesda, MD) and Photoshop (Adobe Systems, San Jose, CA), between 1 and 300 μm . The specific surface area was measured by nitrogen adsorption (ASAP2020, Micromeritics) using ~ 2 g of sample for each group, with one measurement per group.

Mechanical testing

The foamed paste was molded in rubber-molds with dimensions of 6 mm diameter and 13 mm height and four samples were immersed together in 80 mL of PBS. To achieve flat and parallel sides as well as a height of 12 mm, according to the ASTM F451 standard,³² polishing was performed on set samples using a 1200 grit SiC article. The CS was measured on 11 or 12 samples per group using a hydraulic universal materials testing machine (MTS, 858, Bionix Medical Technologies, Toledo, OH) at a cross-head speed of 1 mm/min.

The CS was evaluated against the porosity using a model, previously used for both HA foams⁵ and Portland foams,¹¹ where the effects of micro- and macroporosity are considered separately (see Figure 1). The model is described in Eq. (4), where σ is the CS of the macroporous cement, σ_0 is the CS at zero porosity, ρ/ρ_s is the relative density of the equivalent nonfoamed cement, P is the porosity of the cement (here macroporosity), and m and q are empirical constants. Previous studies by Ginebra et al.⁵ on

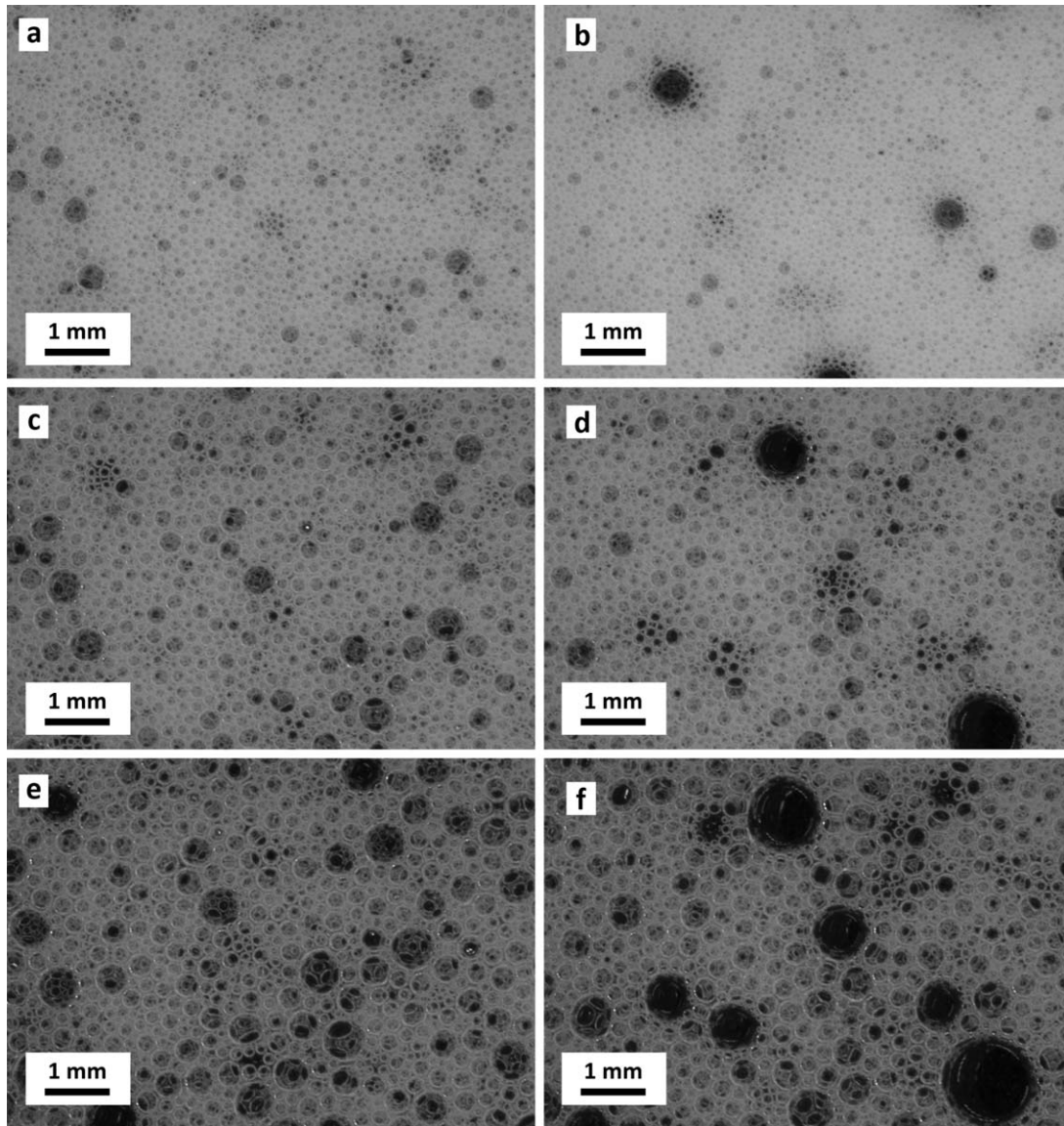


FIGURE 2. Micrographs of liquid foams made from 1 mass% of Tween (a, c, and e) and Pluronic (b, d, and f) in water, 1 (a and b), 3 (c and d), and 6 (e and f) min after foaming.

HA foams have used $m = 2.64$, which seemed to fit the results best. Experimental and theoretical studies on other foams have specified that the value for m should lie between 1 and 2.^{11,33} The value of m was in this study set to two; to both follow theoretical and empirical results.

$$\sigma = \sigma_0(\rho/\rho_s)^m e^{-qP} \quad (4)$$

Statistical analysis

IBM SPSS Predictive Analytics v.21 (IBM, Armonk, NY) was used to perform the statistical analysis. Relative effects of a change in composition, in terms of setting time group (1, 2, and 3 mass% SPP, where 1 mass% SPP was combined with a citric acid solution instead of water), L/P ratio, and type of surfactant (Tween or Pluronic), on the cements' setting

time, CS, and macro- and total porosity were evaluated using a General Linear Model (GLM) analysis. Parameter estimates were calculated for all direct and interactive factors. The critical value (α) was set at 0.05.

RESULTS

Liquid foam characterization

The foamability of the liquid foams was 342 (± 46)% and 311 (± 10)% for Tween and Pluronic, respectively. The bubbles formed in the Tween foam [Figure 2(a)] were slightly larger at the beginning than the bubbles formed in the Pluronic foam [Figure 2(b)]. As shown by the time sequence in Figure 2, both foams underwent the typical foam maturation process, leading to a coarsening of the bubbles. However, whereas after 6 min the bubble size distribution in Tween was quite narrow [between ~ 100 and $500 \mu\text{m}$, Figure 2(e)],

TABLE I. Relative Effects of a Change in Composition on IST, CS, Macro-, and Total Porosity, as Illustrated by GLM Analysis and Regression, Showing Parameter Estimates with Standard Errors Within Parentheses

Parameter	IST (min)		Macroporosity (%)		Total Porosity (%)		CS (MPa)	
	Estimate	p-Value	Estimate	p-Value	Estimate	p-Value	Estimate	p-Value
Intercept	12.9 (0.7)	<0.001	55.8 (3.2)	<0.001	76.3 (1.6)	<0.001	0.86 (0.26)	0.001
1 mass% SPP + 0.5 M CA	26.9 (1.2)	<0.001	28.6 (5.1)	<0.001	9.8 (2.7)	<0.001	-1.06 (0.47)	0.025
3 mass% SPP	8.9 (0.8)	<0.001	7.2 (3.4)	0.036	2.1 (1.7)	0.206	-0.70 (0.32)	0.029
<i>L/P</i> = 0.37	-12.7 (1.5)	<0.001	-54.3 (6.8)	<0.001	-31.2 (3.4)	<0.001	6.05 (0.59)	<0.001
<i>L/P</i> = 0.40	-12.4 (1.5)	<0.001	-40.5 (6.8)	<0.001	-20.4 (3.4)	<0.001	3.86 (0.59)	<0.001
<i>L/P</i> = 0.43	-6.1 (1.2)	<0.001	-28.2 (5.1)	<0.001	-11.7 (2.6)	<0.001	1.92 (0.48)	<0.001
<i>L/P</i> = 0.45	-3.4 (0.9)	<0.001	-19.2 (4.3)	<0.001	-11.4 (2.1)	<0.001	0.95 (0.35)	0.008
<i>L/P</i> = 0.47	-2.6 (0.9)	0.003	-12.7 (4.3)	0.005	-4.3 (2.2)	0.051	0.77 (0.35)	0.031
Pluronic	5.7 (0.9)	<0.001	-16.7 (4.2)	<0.001	-5.4 (2.1)	0.012	0.84 (0.37)	0.024
1 Mass% SPP + 0.5 M CA • Pluronic	NS	NS	NS	NS	NS	NS	-2.14 (0.62)	0.01
3 Mass% SPP • Pluronic	NS	NS	8.1 (3.9)	0.039	5.5 (1.9)	0.007	-0.79 (0.37)	0.033
<i>L/P</i> = 0.37 • Pluronic	-7.7 (2.1)	<0.001	NS	NS	NS	NS	3.16 (0.81)	<0.001
<i>L/P</i> = 0.40 • Pluronic	-6.6 (2.1)	0.001	18.9 (9.0)	0.040	NS	NS	1.69 (0.81)	0.038
<i>L/P</i> = 0.43 • Pluronic	-8.7 (1.6)	<0.001	NS	NS	NS	NS	1.36 (0.63)	0.033
<i>L/P</i> = 0.45 • Pluronic	-5.1 (1.2)	<0.001	NS	NS	NS	NS	1.13 (0.49)	0.022
<i>L/P</i> = 0.47 • Pluronic	-5.1 (1.2)	<0.001	NS	NS	-6.7 (2.7)	0.018	NS	NS

T-0.50-2-W (i.e., 2 mass% SPP, *L/P* = 0.50 mL/g, and Tween) corresponds to the intercept, that is, any other combination could lead to a decrease or increase of the predicted parameter value, depending on coefficient significance. For example, 2 mass% SPP, *L/P* = 0.50 mL/g, and Tween® 80 would give a predicted IST of 12.9 min (intercept), whereas if Pluronic was used instead of Tween, while maintaining 2 mass% SPP and *L/P* = 0.50 mL/g, the predicted IST would be 12.9 + 5.7 = 18.6 min (intercept + direct effect of Pluronic). NS denotes nonsignificance at the 0.05 level.

some larger bubbles, with a diameter up to around 1 mm, were seen in the Pluronic foam [Figure 2(f)] giving a broader bubble size distribution.

Setting time

The IST differed significantly with SPP content, with cements containing 1 mass% SPP and citric acid, as well as cements containing 3 mass% SPP giving longer setting times than cements containing 2 mass% SPP. (Table I). The *L/P* strongly influenced the setting time, with shorter setting times observed for lower *L/P* (Figure 3, Table I). This effect was even more pronounced when Pluronic was used instead of Tween (Table I).

Porosity and microstructure

The skeletal density measured with helium pycnometry was 2.46 (± 0.09), and 2.58 (± 0.04) g/cm³ for samples containing Tween and Pluronic, respectively. Furthermore, the apparent densities of the non-foamed samples were all between 1.2 and 1.6 g/cm³.

The statistical analysis of both macro- and total porosity showed comparable results: the foams containing 1 mass% SPP gave significantly higher porosities than the foams containing 2 or 3 mass% SPP (Table I). Furthermore, the *L/P* clearly affected the porosity, with higher porosities for higher *L/P* (Table I). Additionally, foams containing Pluronic gave significantly lower macroporosity than the Tween foams (Table I), except for 3 mass% SPP. Pluronic foams appeared to reach a maximum in total porosity of ~70%, while no such maximum was seen for the Tween foams (Figure 4). For both surfactants, the largest range in macroporosity was found for the cements containing 1 mass%

SPP, with 30–56% for Tween and 22–48% for Pluronic. The highest porosity was achieved for samples T-0.43-1-C and T-0.50-2-W, which both had total porosities of 76% and macroporosities of 56%. These were in fact the highest *L/P* tested for the respective setting retardants combinations.

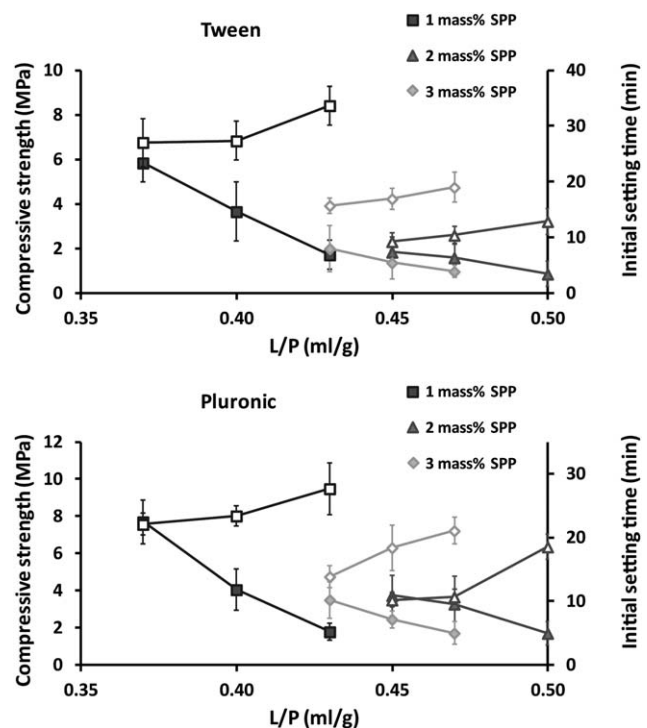


FIGURE 3. CS and IST plotted against the *L/P* ratio used. CS is plotted with filled markers, and IST is plotted with unfilled markers. Error bars indicate standard deviations.

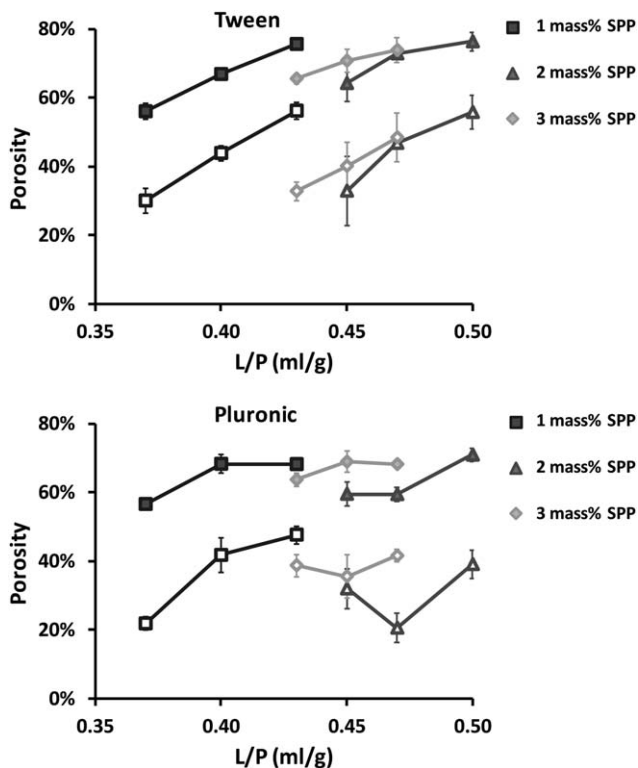


FIGURE 4. Porosity of samples plotted against the L/P ratio used. Total porosity is plotted with filled markers, and macroporosity is plotted with unfilled markers. Error bars indicate standard deviation for $n = 11$ or 12 .

From the SEM micrographs of Tween samples, it can be noted that a high L/P gave more and better distributed macropores (Figure 5). The pores in the cement containing 2 mass% SPP (Figure 5d) appeared slightly smaller than the pores in the cements containing 1 and 3 mass% SPP [Figure 5(b,f)]. Sample T-0.47-3-W was very brittle, which is visible to the left in the micrograph [Figure 5(f)] where the sample broke during SEM sample preparation. The interconnections, seen in the SEM micrograph of this sample, were quite large, ranging around $150\ \mu\text{m}$. Sample T-0.43-1-C [Figure 5(b)] had an average pore size of $\sim 200\text{--}300\ \mu\text{m}$ with interconnections in the range of $100\ \mu\text{m}$, while sample T-0.50-2-W [Figure 5d] contained pores ranging between 100 and $200\ \mu\text{m}$, with interconnections of around $50\ \mu\text{m}$. Samples with the lower L/P did not have as many interconnections and the ones that could be observed were small [$<50\ \mu\text{m}$, Figure 5(a,c,e)]. In samples containing Pluronic, it was difficult to identify a clear trend (Figure 6). It was, however, clear that the macropores formed in the Pluronic samples were smaller, with a less even distribution compared with the pores formed in the Tween samples. Furthermore, the interconnections in these samples were small ($<50\ \mu\text{m}$, Figure 6).

Since 1 mass% SPP in general, and coupled with the surfactant Tween in particular, gave the most promising porosity results it was decided to run MIP and image analysis on the samples with the highest and the lowest L/P ratio within this group. The total porosities for these samples were found to be 52 and 63%, with 24 and 43% pores >5

μm for T-0.37-1-C and T-0.43-1-C, respectively. The pore distribution is illustrated in Figure 7(a).

From the image analysis it was found that the average interconnection size for T-0.37-1-C and T-0.43-1-C was 145 and $172\ \mu\text{m}$, respectively, and that the amount of interconnections was 1.3% and 3.6% of the area analyzed. A comparison between MIP and image analysis showed that MIP gave slightly smaller pore entrance sizes [Figure 7(b)]. It was furthermore seen that the relative amounts found were consistent between both analysis methods, with T-0.43-1-C giving approximately twice the frequency as T-0.37-1-C.

The SEM micrographs, inserts in Figures 5 and 6, indicate that the crystals formed when using citric acid as the liquid were more sheet like and slightly larger than those formed when using water. Nonetheless, the specific surface area was around $1\ \text{m}^2/\text{g}$ for all compositions, with the samples made with Pluronic having slightly higher surface area than samples made with Tween. However, with such small surface area values the precision obtained when using nitrogen as an adsorbate is low. Therefore, no further conclusions can be drawn from the data.

Mechanical properties

The CS varied between ~ 1 and $8\ \text{MPa}$ for the foamed cements 3. Most of the brushite foams had strengths below $5\ \text{MPa}$. The highest strengths were found for the cements with the lowest L/P ratio, that is, compositions T/P-0.37-1-C with a CS of $5.8 (\pm 0.9)$ and $7.7 (\pm 1.2)\ \text{MPa}$ for Tween and Pluronic, respectively. In fact, the CS increased with decreasing L/P ratio (3, Table I). The statistical analysis of CS showed that there was a significant effect of cement composition. Both the 1 mass% group (containing citric acid) and the 3 mass% group were predicted to give a lower CS than the 2 mass% group. There was furthermore a significant difference between the two surfactants used, with Pluronic giving stronger cements for the 2 mass% SPP containing cements (Table I). However, when evaluating the CS/porosity dependence according to Eq. (4) it was observed that cements containing 1 mass% SPP had higher strengths relative to the porosity, compared with cements containing 2 and 3 mass% SPP (Figure 8). Since a different liquid (citric acid instead of water) was used for the samples containing 1 mass% SPP, which had a strong effect on the grain morphology (as previously discussed, section "Porosity and microstructure" and Figures 6 and 7), the CS/porosity relationship for 1 mass% SPP was evaluated separately from 2 and 3 mass%. Both Tween and Pluronic containing foams gave σ_0 values of $22\text{--}23\ \text{MPa}$ for 2 and 3 mass% SPP, while 1 mass% showed higher values for both surfactants, 50 and $92\ \text{MPa}$ for Tween and Pluronic, respectively (Table II). The q value was found to lie between 3.7 and 3.9 for Tween foams, while a bigger variation was seen for Pluronic foams with 5.6 for 1 mass% SPP and 2.7 for 2 and 3 mass% SPP foams.

DISCUSSION

The results presented herein show that it is indeed possible to produce highly porous brushite foams with a total

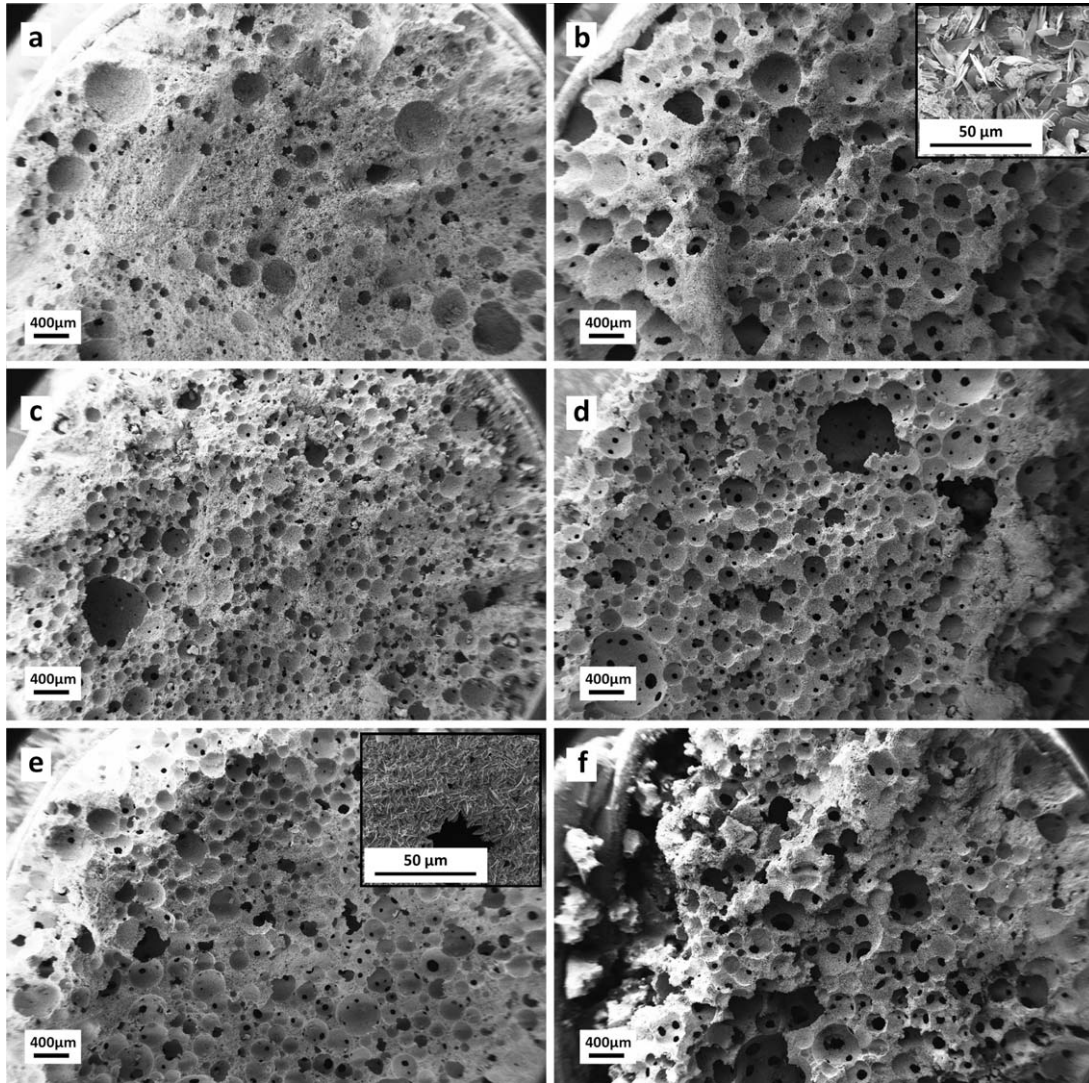


FIGURE 5. SEM micrographs of Tween samples (a) T-0.37-1-C, (b) T-0.43-1-C, (c) T-0.45-2-W, (d) T-0.50-2-W, (e) T-0.43-3-W, and (f) T-0.47-3-W. Inserts are showing a higher magnification of one sample with, and one without citric acid.

porosity of up to 75% and a macroporosity above 55%. These values are within the maximum volume percentage of air within a liquid foam,³⁰ and are similar to what has previously been presented for HA cements prepared both by a foaming technique and by using a sacrificial phase.^{3,5-8,12,13,21,25}

Generally, surfactants stabilize foams at the water-air interface, by lowering the energies required to maintain the larger interfacial area associated with the formation of air bubbles.³⁰ Although the stability of these foams is much higher than the stability of a water-air interface without added surfactants, the process of foam maturation, which is controlled by drainage, coalescence of neighboring bubbles and Ostwald ripening, must still be taken into account.³⁰ Drainage occurs when water in the lamella between bubbles sink to the bottom due to the force of gravity, and separation of the foam, into a highly porous and a less porous part, will then appear. A rupture of the lamella between bubbles can occur due to drainage, which will cause a thin-

ning of the lamella between bubbles, or due to poor stabilization capacity of the surfactant. The rupture will result in coalescence of two neighboring bubbles. Ostwald ripening is a process whereby a coarsening of bubbles occurs through a gas diffusion process caused by the pressure differences between small and large bubbles.³⁴ When powder is introduced to the liquid foam the viscosity increases, which prevents, or at least slows down, both drainage and gas diffusion between bubbles and is, therefore, expected to delay the foam maturation process.³⁴ In this respect it should be noted that the brushite foams had larger bubbles than the corresponding liquid foams after 1 minute of foaming (corresponding to the time when the powder was incorporated into the liquid foam; Figure 2). This suggests that the maturation process was not completely hindered by the addition of the powder, and that some foam maturation took place either in the mixing step or after mixing and before cement setting. This effect was more pronounced in

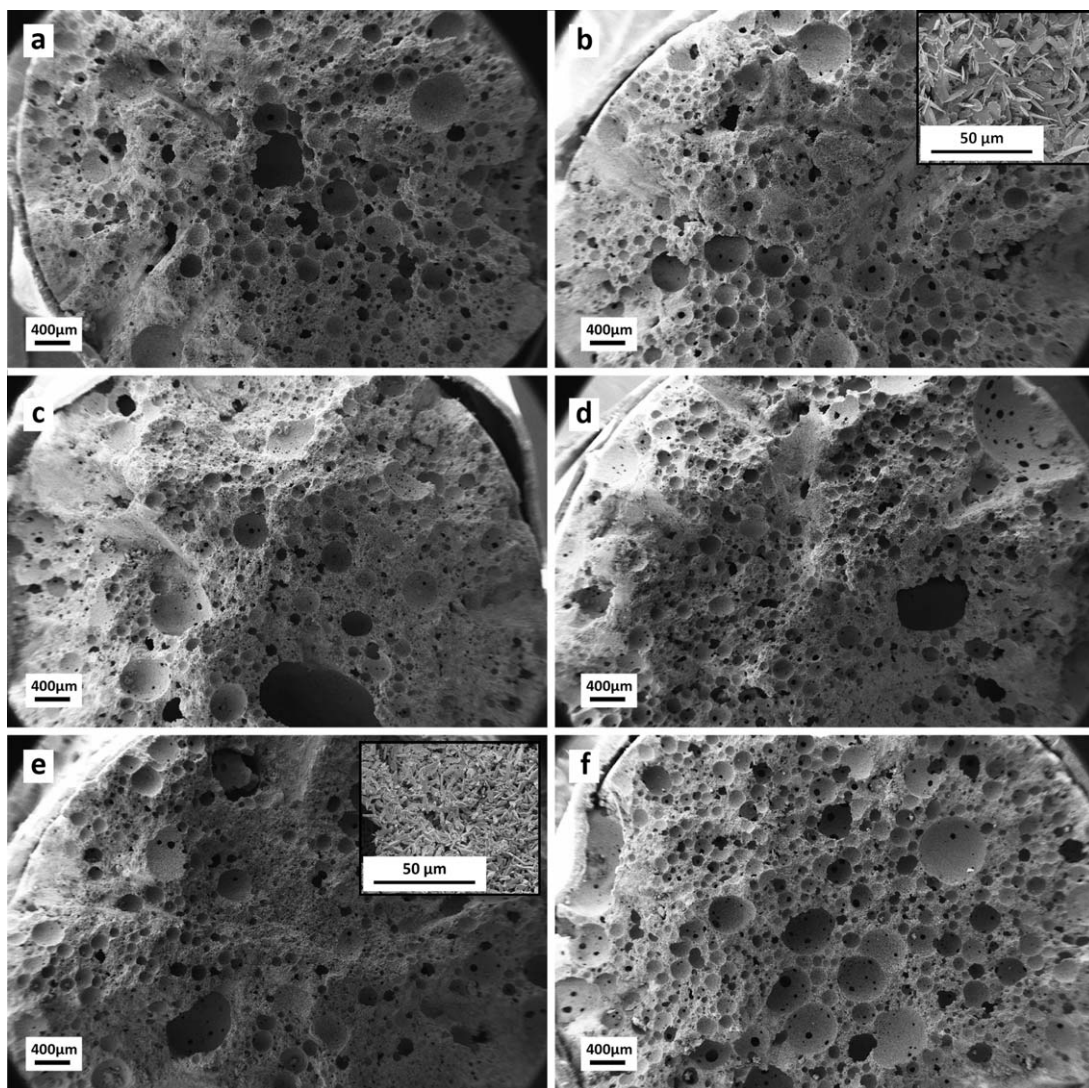


FIGURE 6. SEM micrographs of Pluronic samples (a) P-0.37-1-C, (b) P-0.43-1-C, (c) P-0.45-2-W, (d) P-0.50-2-W, (e) P-0.43-3-W, and (f) P-0.47-3-W. Inserts are showing a higher magnification of one sample with, and one without citric acid.

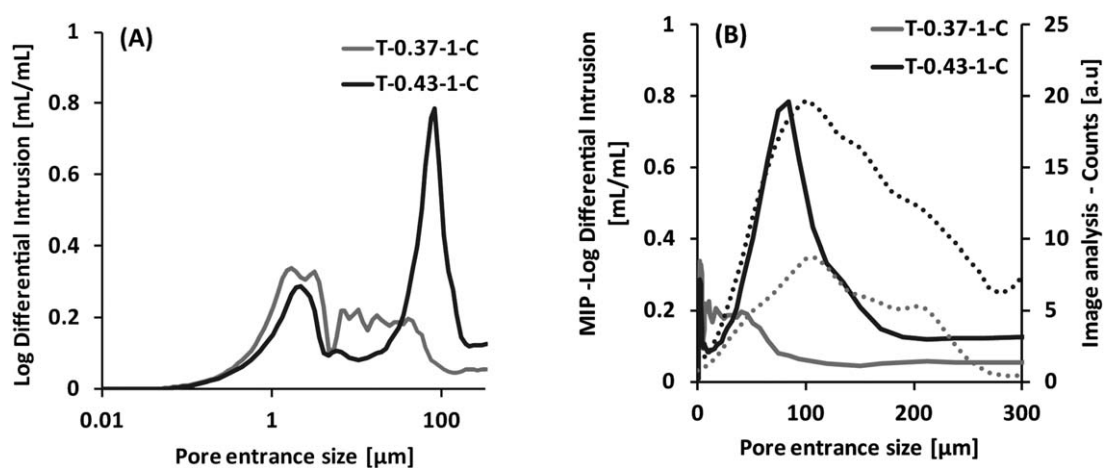


FIGURE 7. (a) Pore entrance size distribution as measured with MIP on samples T-0.37-1-C and T-0.43-1-C. (b) Comparison of the results of pore interconnections from image analysis (dotted lines) and MIP (solid lines) on samples T-0.37-1-C and T-0.43-1-C.

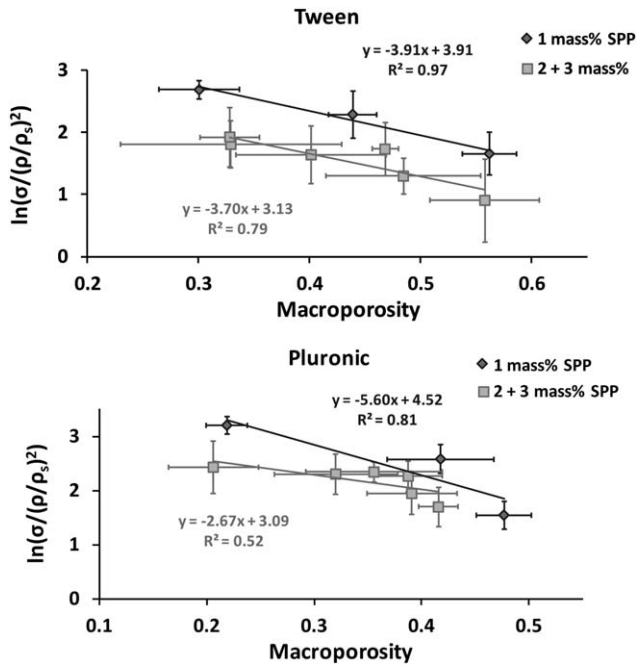


FIGURE 8. CS and porosity results evaluated with Eq. (4). $\ln(\sigma/(\rho/\rho_s)^m)$ (with $m=2$) is plotted against P . The equation of the trend line is then given as $y = -qP + \ln(\sigma_0)$.

the foams prepared with large L/P [Figures 5 and 6; (a,c,e) vs. (b,d,f)]. When a smaller amount of powder was added to the liquid foam, there was likely not enough powder present to reduce the drainage of the liquid and both the coalescence of neighboring bubbles and Ostwald ripening could occur to a higher degree, resulting in larger bubble sizes.

To obtain the highest foamability possible Tween and Pluronic were used as foaming agents at a concentration considerably higher than their critical micelle concentration (1.2×10^{-5} M for Tween³⁵ and 6.9×10^{-5} M for Pluronic³⁶). The foamabilities observed for both surfactants were similar ($342 (\pm 46)\%$ for Tween and $311 (\pm 10)\%$ for Pluronic, corresponding to a porosity of 71 and 68%, respectively) at the concentrations and foaming conditions studied. Since the brushite foam is derived from the liquid foam a similar amount of macroporosity was expected in the two types of foams, and this was indeed observed for cements containing 1 and 3 mass% SPP. It was furthermore observed that foams prepared with Pluronic seemed to have a maximum total porosity of $\sim 70\%$, while no such maximum was observed for foams prepared with Tween. However, it is likely that such a maximum would be observed also for the Tween containing foams at slightly higher L/P than those investigated here. Tween generally gave larger and more homogeneously distributed macropores compared with the cements prepared with Pluronic, which is in agreement with previous studies that show that the surfactant used highly influences the bubble size.³⁷ This difference in macropore size could furthermore come from the mixing of the liquid foam with the cement powder. In fact, in contrast to Tween, the viscosity of Pluronic increases with an increment in temperature.^{28,29} Although the concentration of

Pluronic used is not enough to gel at body temperature, a small increase in temperature due to the brushite cement setting could produce an increase of the viscosity of the continuous phase of the liquid foam, requiring greater shear stresses to incorporate the powder into the foam, resulting in rupture of bubbles as a side effect. In agreement with this, the macropores seen in the Tween cements seemed to better preserve their spherical shape during sample preparation and setting.

A higher porosity was achieved in brushite foam compositions with the longest IST, when two compositions with the same L/P were compared (Figure 4). When the liquid foam is mixed with the powder the dissolution-precipitation reaction is started.²⁵ Depending on the rate of the precipitation reaction; that is, the rate of crystal formation, crystal growth, and crystal aggregation, the rate of paste thickening and solidifying varies. In a regular cement, if mixing or molding is performed after the crystals have started to entangle and aggregate, the aggregates might be disrupted and the cement weakened. Furthermore, for the foamed cements, this means that the microstructure is damaged and cement solidifying around macropores is ruptured while the pores are being cleaved open or deformed, and a compaction of the paste is more easily achieved [Figures 5(a) and 6(a,c,e)]. The fast setting cements might therefore attain a lower final macroporosity compared with the cements where the setting starts first after molding. Although a longer setting time thus is preferred, it should be noted that there might be a counteractive effect of a prolonged IST related to an access of drainage and coalescence of macropores. The IST should therefore be kept long enough to prevent compaction during molding, but short enough to prevent drainage and a high degree of foam maturation. The structural analysis with SEM showed, especially for Tween samples, that a higher L/P resulted in a better distribution of macropores and, in general, larger macropores, when the SPP content was kept the same (Figures 5 and 6). Although the powder added should supposedly not affect the foam, a rupture of the bubbles due to the powder weight could be seen during incorporation of powder into the liquid foam. The use of more powder (i.e., lower L/P ratio) would hence affect the liquid foam to a greater extent, and could in some cases result in regions of cement without macropores. Furthermore, the longer IST together with the normal occurrence of a higher porosity at higher L/P ^{22,25,38,39} might also contribute to a higher macroporosity.

In the SEM micrograph for T-0.43-1-C the pore size of the macropores was found to lie around 200–300 μm with interconnections of around 100 μm , which means that these

TABLE II. Summary of Constants Achieved from Evaluation of CS and Porosity Results with [Eq. (4); Figure 8]

Sample	σ_0	q
1 mass% SPP Tween® 80	50	3.9
2 and 3 mass% SPP Tween® 80	23	3.7
1 mass% SPP Pluronic® F-127	92	5.6
2 and 3 mass% SPP Pluronic® F-127	22	2.7

foams could present an optimal situation for bone ingrowth⁴ [Figure 5(b)]. MIP, however, showed pore entrance sizes of around 80 μm (Figure 7). Since pores, when intruded with mercury, are only accessed through their entrances/interconnections, the results obtained with MIP do not represent the actual pore size but the size of the pore entrance, meaning that the pore is generally larger than what is seen with MIP. This phenomenon, which is referred to as the ink bottle-effect, was studied by Lange et al., who showed that the actual pore size was about three times the size of the pore entrance sizes measured with MIP,⁴⁰ which is in agreement with the current findings. Furthermore, when comparing the entrance/interconnectivity sizes achieved with MIP and image analysis, it was found that image analysis gave slightly larger entrance/interconnectivity sizes [Figure 7(b)]. This is due to the presence of interconnected pore networks. When a larger pore is interconnected to a smaller pore, the throat diameter of the smaller pore will also be considered the throat diameter of the second, larger, pore. The larger pore will then appear to have the same diameter as the smaller pore, that is, the volume of smaller pores will have greater weight and the amount of large pores have less weight in the final porosity value than what is truly the case.⁴¹

When analyzing the SEM micrographs, larger crystals were observed in the samples containing citric acid than in those obtained with water as the liquid (Figures 5 and 6). However, the specific surface area measured for all foams here was around 1 m^2/g . This indicates that the crystals in the samples made with citric acid, although seemingly large, are very thin, resulting in the same specific surface area as with water. A specific surface area of 1 m^2/g is lower or in the same range as what has been presented for HA foams (1–20 m^2/g).^{5,6,12} The CS, however, was found to be similar to^{5,21,25} or slightly higher than⁶ HA foams with similar porosities. When the CS-porosity relationship was evaluated it was found that the predicted value of σ_0 differed substantially between the investigated foams. Tween showed a lower σ_0 than Pluronic for the group containing 1 mass% SPP (50 and 92 MPa for Tween and Pluronic, respectively). Similar compositions without added surfactant, have shown values of 74 MPa for samples with a microporosity of $\sim 13\%$.²³ If using the achieved values for σ_0 to calculate the theoretical strength for a material with 13% microporosity (i.e., relative density = 0.87, and $P = 0$), strengths of 38 and 70 MPa for Tween and Pluronic, respectively, are achieved. These results indicate that Tween affects the strength negatively, while Pluronic does not have any significant effect on strength. However, Tween proved superior to Pluronic in terms of producing brushite foams with a higher macroporosity, a more homogeneous distribution of macropores, and a higher strength. Furthermore, σ_0 is calculated from the exponential of the constant of the regression line, meaning that a small change in the line equation results in a large change in σ_0 . It was also seen that the q value differed somewhat between Tween and Pluronic when 1 mass% SPP was used, being 3.91 and 5.60 for Tween and Pluronic, respectively. Values of q have previously been discussed by

Tonyan and Gibson who concluded that q should be between 3 and 6,¹¹ indicating that the model describes the results accurately. The foams containing 2 and 3 mass% SPP showed very similar results with σ_0 values around 22 MPa; which is reasonable for cements without citric acid in the liquid.²² While 1 mass% SPP + 0.5M citric acid was found to give lower strengths than 3 mass% SPP for the same L/P ratio (Figure 3, Table I), the presence of citric acid also increased the porosity, giving rise to a higher strength for a specific porosity. Two cements had the same total porosity (76%) and macroporosity (56%), the strength of the citric acid containing foam (T-0.43–1-C) was 1.7 MPa, while the strength of the cement with water in the liquid (T-0.50–2-W) only was 0.9 MPa (and very fragile). Previous reports have shown that citric acid increases the strength of cements and, thus, the higher strength observed in cements containing citric acid is not surprising.^{42,43}

The brushite foams show promising results for future clinical applications (e.g., bone void filling, or scaffolds for *in vitro* bone generation). However, the *in vivo* behavior and degradation rate have not yet been investigated and although previous publications indicate that the studied foams should have a good *in vivo* behavior^{1,2,44} and a fast degradation rate,^{17–19} this needs to be confirmed in further studies.

CONCLUSIONS

Brushite foams can be created with porosities and CSs similar to those of precipitated HA foams previously reported. Brushite foams containing the surfactant Tween showed more promising micro- and macrostructures compared with foams made from Pluronic. Furthermore, it was seen that the use of two retardants (1 mass% disodium dihydrogen pyrophosphate and 0.5M citric acid) resulted in foams where a high porosity could be achieved, while maximizing the strength, compared with the formulations where water was used in the liquid. The maximum porosity achieved was 76% (total) and 56% (macro), for two groups: Tween containing foams with an L/P of 0.43, 1 mass% SPP and citric acid in the liquid, and Tween containing foams with an L/P of 0.50, 2 mass% SPP and water in the liquid. However, the sample containing citric acid showed better mechanical properties with a CS of 1.7 (± 0.6) MPa. Although these brushite foams show promising results for future clinical use, thorough *in vitro* and *in vivo* evaluations still need to be performed.

ACKNOWLEDGMENTS

The authors are grateful to D. Pastorino for his help with image analysis and M. Pujari-Palmer for proof-reading.

REFERENCES

1. Lee DW, Kim JY, Lew DH. Use of rapidly hardening hydroxyapatite cement for facial contouring surgery. *J Craniofac Surg* 2010; 21:1084–1088.
2. Wolff KD, Swaid S, Nolte D, Bockmann RA, Holzle F, Muller-Mai C. Degradable injectable bone cement in maxillofacial surgery: Indications and clinical experience in 27 patients. *J Craniomaxillofac Surg* 2004;32:71–79.

3. del Valle S, Mino N, Munoz F, Gonzalez A, Planell JA, Ginebra MP. In vivo evaluation of an injectable macroporous calcium phosphate cement. *J Mater Sci Mater Med* 2007;18:353–361.
4. Karageorgiou V, Kaplan D. Porosity of 3D biomaterial scaffolds and osteogenesis. *Biomaterials* 2005;26:5474–5491.
5. Ginebra M-P, Delgado J-A, Harr I, Almirall A, Del Valle S, Planell JA. Factors affecting the structure and properties of an injectable self-setting calcium phosphate foam. *J Biomed Mater Res Part A* 2007;80A:351–361.
6. Barralet JE, Grover L, Gaunt T, Wright AJ, Gibson IR. Preparation of macroporous calcium phosphate cement tissue engineering scaffold. *Biomaterials* 2002;23:3063–3072.
7. Xu HHK, Weir MD, Burguera EF, Fraser AM. Injectable and macroporous calcium phosphate cement scaffold. *Biomaterials* 2006;27:4279–4287.
8. Takagi S, Chow LC. Formation of macropores in calcium phosphate cement implants. *J Mater Sci Mater Med* 2001;12:135–139.
9. Habraken WJEM, Wolke JGC, Mikos AG, Jansen JA. Injectable PLGA microsphere/calcium phosphate cements: Physical properties and degradation characteristics. *J Biomater Sci Polym Ed* 2006;17:1057–1074.
10. Link DP, van den Dolder J, van den Beucken JJJP, Habraken W, Soede A, Boerman OC, Mikos AG, Jansen JA. Evaluation of an orthotopically implanted calcium phosphate cement containing gelatin microparticles. *J Biomed Mater Res Part A* 2009;90A:372–379.
11. Tonyan TD, Gibson LJ. Structure and mechanics of cement foams. *J Mater Sci* 1992;27:6371–6378.
12. Perut F, Montufar EB, Ciapetti G, Santin M, Salvage J, Traykova T, Planell JA, Ginebra MP, Baldini N. Novel soybean/gelatine-based bioactive and injectable hydroxyapatite foam: Material properties and cell response. *Acta Biomater* 2011;7:1780–1787.
13. Montufar EB, Traykova T, Schacht E, Ambrosio L, Santin M, Planell JA, Ginebra M-P. Self-hardening calcium deficient hydroxyapatite/gelatine foams for bone regeneration. *J Mater Sci Mater Med* 2010;21:863–869.
14. Cama G, Gharibi B, Sait MS, Knowles JC, Lagazzo A, Romeed S, Di Silvio L, Deb S. A novel method of forming micro-and macroporous monetite cements. *J Mater Chem B* 2013;1:958–969.
15. Cama G, Barberis F, Botter R, Cirillo P, Capurro M, Quarto R, Scaglione S, Finocchio E, Mussi V, Valbusa U. Preparation and properties of macroporous brushite bone cements. *Acta Biomater* 2009;5:2161–2168.
16. Åberg J, Engstrand Unosson J, Engqvist H. Setting mechanisms of an acidic premixed calcium phosphate cement. *Bioceramics Dev Appl* 2013;3:1–6.
17. Kokubo T. *Bioceramics and their clinical applications*. Woodhead Publishing Limited; 2008.
18. Apelt D, Theiss F, El-Warrak AO, Zlinszky K, Bettschart-Wolfisberger R, Bohner M, Matter S, Auer JA, von Rechenberg B. In vivo behavior of three different injectable hydraulic calcium phosphate cements. *Biomaterials* 2004;25:1439–1451.
19. Grossardt C, Ewald A, Grover LM, Barralet JE, Gbureck U. Passive and active in vitro resorption of calcium and magnesium phosphate cements by osteoclastic cells. *Tissue Eng Part A* 2010;16:3687–3695.
20. Marolt D, Knezevic M, Vunjak-Novakovic G. Bone tissue engineering with human stem cells. *Stem Cell Res Therapy* 2010;1:10.
21. Almirall A, Larrecq G, Delgado JA, Martínez S, Planell JA, Ginebra MP. Fabrication of low temperature macroporous hydroxyapatite scaffolds by foaming and hydrolysis of an α -TCP paste. *Biomaterials* 2004;25:3671–3680.
22. Engstrand J, Persson C, Engqvist H. The effect of composition on mechanical properties of brushite cements. *J Mech Behav Biomed Mater* 2014;29:81–90.
23. Unosson J, Engqvist H. Development of a resorbable calcium phosphate cement with load bearing capacity. *Bioceramics Dev Appl* 2014;4:1–4.
24. Montufar EB, Traykova T, Planell JA, Ginebra M-P. Comparison of a low molecular weight and a macromolecular surfactant as foaming agents for injectable self setting hydroxyapatite foams: Polysorbate 80 versus gelatine. *Mater Sci Eng C* 2011;31:1498–1504.
25. Montufar EB, Traykova T, Gil C, Harr I, Almirall A, Aguirre A, Engel E, Planell JA, Ginebra MP. Foamed surfactant solution as a template for self-setting injectable hydroxyapatite scaffolds for bone regeneration. *Acta Biomater* 2010;6:876–885.
26. Floyd AG. Top ten considerations in the development of parenteral emulsions. *Pharm Sci Technol Today* 1999;2:134–143.
27. Porter MR. *Handbook of surfactants*; 1994.
28. Escobar-Chavez JJ, Lopez-Cervantes M, Naik A, Kalia YN, Quintanar-Guerrero D, Ganem-Quintanar A. Applications of thermo-reversible pluronic F-127 gels in pharmaceutical formulations. *J Pharm Pharm Sci* 2006;9:339–358.
29. Alexandridis P, Alan Hatton T. Poly(ethylene oxide)-poly(propylene oxide)-poly(ethylene oxide) block copolymer surfactants in aqueous solutions and at interfaces: Thermodynamics, structure, dynamics, and modeling. *Colloids Surf A* 1995;96:1–46.
30. Schramm LL. *Emulsions, Foams, and Suspensions-Fundamentals and Applications*. Wiley-VCH Verlag GmbH & Co; 2005.
31. Standard Test Method for Time of Setting of Hydraulic-Cement Paste by Gillmore Needles. ASTM C266-99: ASTM International; 1999.
32. ASTM. Standard Specification for Acrylic Bone Cement. ASTM F451: ASTM International; 2008.
33. Gibson LJ, Ashby MF. The mechanics of three-dimensional cellular materials. *Proc R Soc London A* 1982;382:43–59.
34. Studart AR, Gonzenbach UT, Tervoort E, Gaukler LJ. Processing routes to macroporous ceramics: A review. *J Am Ceram Soc* 2006;89:1771–1789.
35. Sigma. Available at: http://www.sigmaaldrich.com/content/dam/sigma-aldrich/docs/Sigma/Product_Information_Sheet/1/p5188pis.pdf. Accessed on November 6, 2013.
36. Sezgin Z, Yuksel N, Baykara T. Preparation and characterization of polymeric micelles for solubilization of poorly soluble anticancer drugs. *Eur J Pharm Biopharm* 2006;64:261–268.
37. Adkins SS, Chen X, Chan I, Torino E, Nguyen QP, Sanders AW, Johnston KP. Morphology and stability of CO₂-in-water foams with nonionic hydrocarbon surfactants. *Langmuir* 2010;26:5335–5348.
38. Hofmann MP, Mohammed AR, Perrie Y, Gbureck U, Barralet JE. High-strength resorbable brushite bone cement with controlled drug-releasing capabilities. *Acta Biomater* 2009;5:43–49.
39. Gbureck U, Spatz K, Thull R, Barralet JE. Rheological enhancement of mechanically activated α -tricalcium phosphate cements. *J Biomed Mater Res B* 2005;73B:1–6.
40. Lange DA, Jennings HM, Shah SP. Image analysis techniques for characterization of pore structure of cement-based materials. *Cement Concr Res* 1994;24:841–853.
41. Leon CALY. New perspectives in mercury porosimetry. *Adv Colloid Interface Sci* 1998;76:341–372.
42. Giocondi JL, El-Dasher BS, Nancollas GH, Orme CA. Molecular mechanisms of crystallization impacting calcium phosphate cements. *Philos Trans A Math Phys Eng Sci* 2010;368:1937–1961.
43. Mariño FT, Torres J, Hamdan M, Rodríguez CR, Cabarcos EL. Advantages of using glycolic acid as a retardant in a brushite forming cement. *J Biomed Mater Res B Appl Biomater* 2007;83B:571–579.
44. Larsson S. Calcium phosphates: What is the evidence? *J Orthop Trauma* 2010;24:41–45.